Transient and Oscillatory Granular Shear Flow

Masahiro Toiya, Justin Stambaugh, and Wolfgang Losert*

Institute for Research in Electronics and Applied Physics, Institute for Physical Science and Technology, and Department of Physics, University of Maryland, College Park, Maryland 20742, USA

(Received 9 October 2003; published 18 August 2004)

The forces and particle motion during transient and oscillatory shear of granular material are investigated experimentally. In a shear cell of Taylor-Couette-type we find that how a granular shear flow starts depends strongly on the prior shear direction. If the shear direction is reversed, the material goes through a transient period during which the material compacts, the shear force is small, and the shear band is wide. Three-dimensional confocal imaging of particle rearrangements during shear reversal shows that bulk and surface flows are comparable. Repeated reversals, or oscillations of the shear direction, lead to additional compaction, which can be described by a stretched exponential, similar to compaction induced by tapping.

DOI: 10.1103/PhysRevLett.93.088001 PACS numbers: 45.70.Mg, 45.70.Cc, 81.05.Rm

How do dense granular materials such as sand and grains rearrange under an applied external force? Controlled initiation of flow of granular matter is essential for transportation of raw materials, and many processes in pharmaceutical, chemical, and food industries. In geological events, the start of granular flow is of particular interest. For example, we have shown that in rock avalanches the prior history of shear forces applied to the soil may play a key role in determining the risk of such catastrophic flows [1]. Various models to describe the steady state flow properties of granular matter have been developed [2–5]. In these models, the state of a system is characterized by density, granular temperature, and pressure. However, it is unclear at what point these models can be applied to describe the initiation of a flow from a granular assembly at rest. In this Letter we investigate how a granular flow starts, and determine that prior shear is a key parameter in flow initiation.

The properties of some flow models under nonsteady conditions have been studied [6]. However, expanding flow models may not be sufficient: The dynamics of granular matter at or close to rest has been shown to depend upon the history of applied forces [7,8]. These experiments showed that density alone is not a sufficient indicator of the future evolution of the system under tapping or shear.

In this Letter we study the effects of prior shear on the dynamics of granular flow. Our apparatus shown in Fig. 1 consists of two concentric cylinders of which the inner cylinder is driven by a variable speed dc servo motor. The outer cylinder is fixed. The gap between the cylinders is filled with glass beads of diameter $d = 1$ or 2 mm to an average bulk height of 92 mm. A layer of glass beads of the same kind that fills the gap is glued to both cylinder surfaces, while the stationary bottom is smooth. Measured flow properties are the width of the shear band (where the motion of particles during shear is most pronounced), the density of the material, and the torque required for shearing. We find history dependence at the start of flow by shearing: Upon reversal of the shear direction, the shear band widens, the material compacts, and the shear strength weakens, gradually recovering steady state flow.

The top surface of the granular material is imaged at up to 500 frames/s with a high speed camera mounted above the shear cell. A torque sensor positioned between the motor and the motor mount monitors the torque exerted by the motor on the inner cylinder. The height is recorded as a measure of average particle density by a camera mounted on the side of the shear cell. In a typical run the inner cylinder is rotated at 6–12 mHz, corresponding to a tangential velocity of 4–8 mm/s.

Prior to the start of each run, the inner cylinder is rotated at a slow steady speed for at least two rotations to prepare the particles in a consistent initial arrangement. Then the inner cylinder is stopped. Shear flow is initiated again by rotating the inner cylinder either in the same or the opposite direction. We found that the start of shear flow is not strongly dependent on shear rate at the low

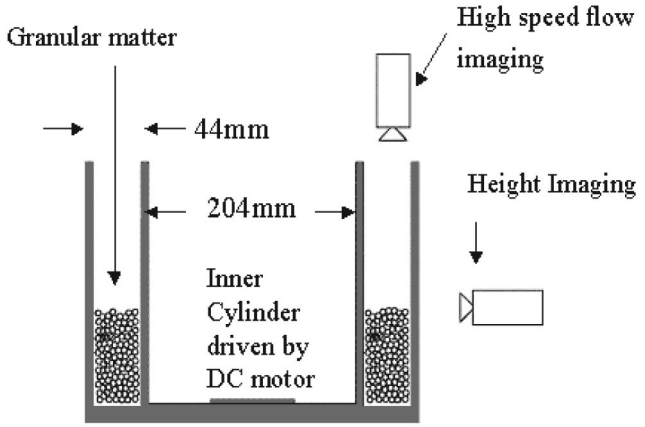

FIG. 1. Schematic of the shear cell.

 0031-9007/04/93(8)/088001(4)$22.50

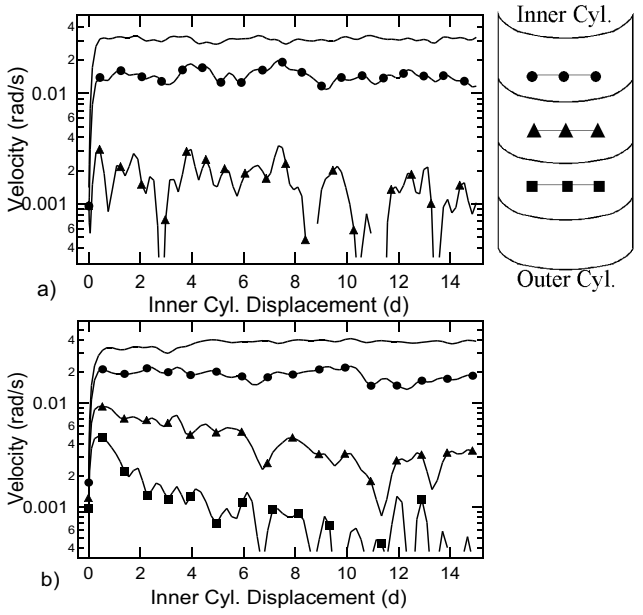

FIG. 2. Average flow velocity of particles $V(r)$ vs shear displacement of the inner cylinder in units of particle diameter d. Lines without markers track the inner cylinder motion. Lines with markers trace average velocities in three regions as labeled in the schematic of the top surface. When shear is restarted in the same direction (a), a steady state is reached immediately. When shear is reversed (b), the shear band is initially wider.

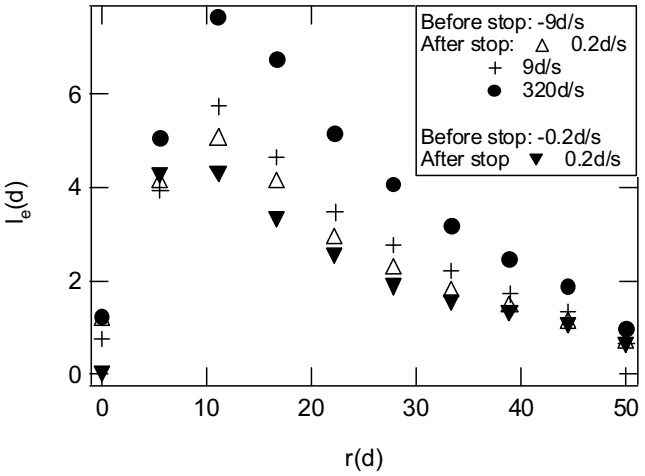

FIG. 3. Extra displacement $l_e(r)$ as a function of distance r from the shear surface. Compared to steady state shear, particles travel extra displacements due to transiently wider shear band after reversal of shear direction.

speeds we investigated (from 0.3 mHz to 0.5 Hz), as had been found for slow steady shear [7,9,10], but that it does depend on the shear direction.

Figure 2 shows the average velocities of particles in the top layer at various distances from the inner cylinder $V(r)$ as a function of shear displacement of the inner cylinder for $d = 2$ mm particles. Each curve represents $V(r)$ averaged over a $5.5d$ wide layer. Figure 2(a) shows that a steady state is reached within $1d$ after the shear cell is started in the same direction as the direction of prior shear. Figure 2(b) shows $V(r)$ after the shear cell was started in the opposite direction. One can see a transient state during which the shear band is wider and particles far from the inner cylinder move appreciably for a shear strain of $(5–10)d$ measured at the inner cylinder.

The transiently wider shear band upon reversal of shear direction means that the particles gain extra displacements compared to the steady state case. The extra displacement $l_e(r)$ of particles during this initial transient state is measured as $l_e(r) = \int [V(r, t) - V_0(r)]dt$ where $V_0(r)$ is the approximate steady state velocity of particles at a distance r reached after a strain of $\sim 10d$. Figure 3 shows l_e as a function of r. $l_e(r)$ increases with the distance from the outer cylinder, except for the layer closest to the shear surface, which does not show significant extra displacement. Maximum extra displacement occurs at $r \approx 12d$ for the particle sizes tested ($d = 1$ and 2 mm). Density measurements indicate that an additional slow transient exists, but the shear band during this slow transient does not differ appreciably from the steady state shear band. $l_e(r)$ is not strongly dependent on shear rates before and after reversal. We also found qualitatively similar results for $V(r)$ and l_e with a bottom connected to

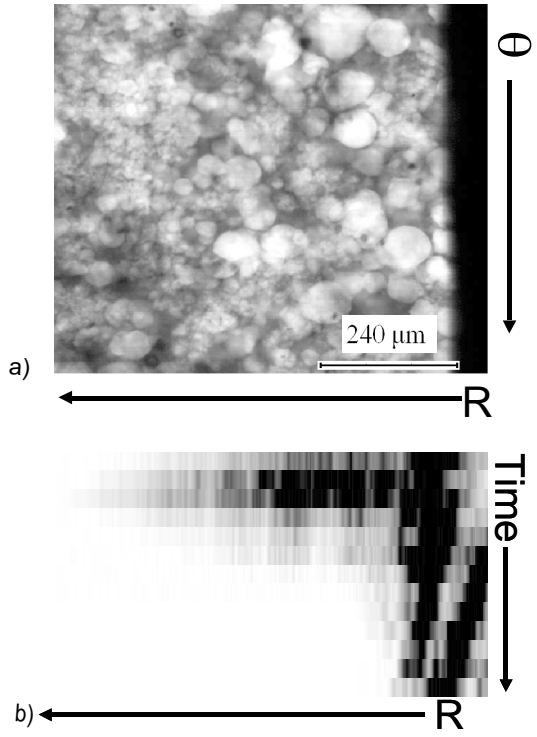

FIG. 4. Confocal image of the cross section through a granular layer $15d$ inside a granular shear flow (a). Spacetime plot of the θ-averaged intensity of difference images, a measure of the extent of the moving region (b).

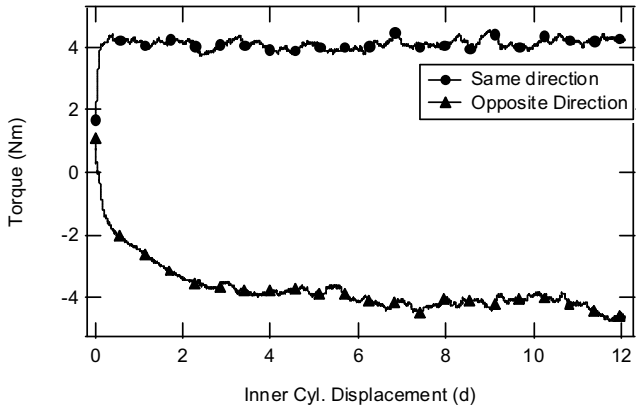

FIG. 5. Shear stress as a function of shear displacement. When the shear direction is reversed, the shear stress takes about (5–10)d to reach a steady state. Same direction plot shown for comparison.

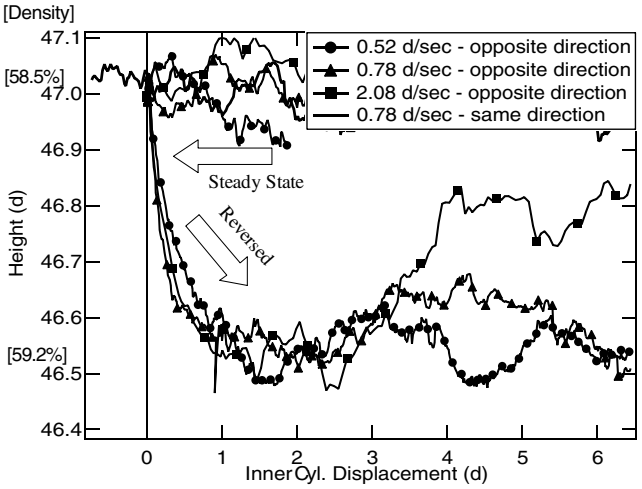

FIG. 6. Column height vs shear displacement. The material compacts over strain of less than one particle diameter and then gradually expands again. Density or volume fraction is shown in square brackets.

the inner cylinder, and when rotating the outer cylinder with the inner cylinder fixed.

Does this surface measurement reflect the flow in the bulk? In order to analyze the 3D structure of grains and shear band widths at various depths in the granular material, a smaller shear cell was used for imaging of the grain interior with a two-photon confocal microscope. The granular material used in the small shear cell is highly polydisperse, amorphous silica beads with an average particle diameter of 30 microns. They are immersed in index matching fluid with 0.5 wt% laser dye Coumarin152 added for fluorescence imaging. Shear flow is imaged through the bottom, about 15d into the material. Figure 4(a) shows an image of the cross section through the granular material about 15d into the material. Figure 4(b) shows a spacetime plot of the intensity of difference images, averaged in the θ direction. This is a qualitative indicator of shear band widths. As on the surface, a transient widening of the shear band is observed. Significantly more widening of the shear band is observed here, either due to the larger number of layers in the shear cell (the apparatus is 170d wide) or due to the polydispersity of the material used in this experiment. Earlier experiments have shown that the steady state velocity profiles on the surface and in the bulk are very similar [10]. Hence, it is not surprising that the flow transient on the surface also reflects bulk behavior.

Figure 5 shows the evolution of torque for stop-start and reversal experiments on the large shear cell as functions of strain represented by the displacement of the inner cylinder. Transient weakening of the shear stress is observed upon reversal. Similar behavior was found for 2D sheared granular matter without compaction [11] and for sheared particles immersed in a density matched fluid [12].

If the strength of the material is a function of its density, one might expect that a weaker state should have lower density. The opposite effect was observed. The height of granular material was measured as an indicator of density (Fig. 1). Figure 6 shows the height of the material during stop-start and reversal experiments on the large shear cell as a function of shear strain. The height remains constant within the experimental error for stop-start experiments. For shear reversal, it drops by 0.4d approximately exponentially over a characteristic shear strain of 0.5d. Measurements were taken in various places around the shear cell to rule out the geometric defects of the apparatus.

Further compaction can be achieved by reversing the shearing direction after compaction has taken place and before the system dilates back to a steady state. We can

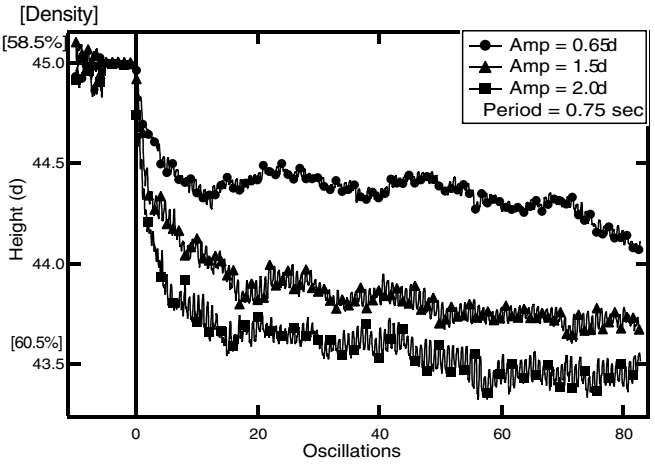

FIG. 7. Density development under repeated shear reversals as a function of the number of oscillations. Reversal of shear is repeated before full recovery takes place, resulting in further compaction.

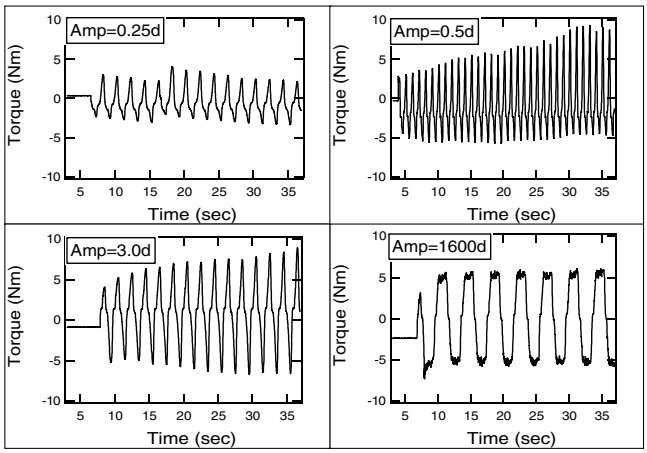

FIG. 8. Shear strain as a function of time. Depending on the amplitude of oscillation, gradual strengthening in both directions was observed.

reverse the shearing direction repeatedly after each height drop (oscillations). Figure 7 shows the average height of the material as a function of time. The amount of compaction during each reversal gradually decreases. The functional form of the density increase can be fit equally well to the logarithmic law developed by Knight *et al.* [13] to describe compaction of granular material under tapping.

A stretched exponential, which may be used to describe the dynamics of jammed systems close to the glass transition as well as the tapped granular material mentioned above [14], also fits the experimental data well. $h(x) = h_\infty + \Delta h \exp[-(\frac{x+x_0}{\tau})^\alpha]$, where x is the number of oscillations. Average values from fits yield $\alpha = 1.6 \pm 0.4$ and $\tau = 6.0 \pm 0.7$. Note that the compaction does not strongly depend on the oscillation amplitude, as long as the oscillation amplitude is larger than the characteristic length of $0.5d$ over which the system compacts during a single reversal (see Fig. 6).

Shear stress develops depending on the amplitude of oscillations as shown in Fig. 8. For small oscillation amplitudes of $0.25d$, the shear stress remains below the steady state stress. For larger amplitudes, the shear stress gradually increases in one direction beyond the shear stress during steady state shear. For larger oscillation amplitudes the shear stress recovers its steady state value in both directions. Our results indicate that repeated reversals before reaching steady state gradually strengthen the material. Qualitatively this is consistent with the compaction of the material.

In summary, we find that the direction of prior shear influences how granular matter starts to flow. If shear flow is started in the same direction as prior shear, the system reaches a steady state flow with minimal strain of less than one particle diameter (d). If the shear direction is reversed, the material compacts by a fraction of a particle diameter over a characteristic strain of $0.5d$. Also upon reversal, material far from the shear surface flows significantly more than in the steady state, and the shear stress is reduced, both over a characteristic strain of $(5–10)d$.

The anisotropy of the contact network has been seen in 2D experiments, where the shear stress and particle contacts can be visualized with birefringent disks [9], but where the density of the system is constant. Our experiments show that strong *macroscopic* effects result from this anisotropy which are observable during the onset of shear flow. Those effects provide an indirect measure of the anisotropy of the configuration of a granular assembly at rest under shear stress. In our 3D system, the characteristic strain over which the system compacts indicates that particles need to move by up to $1d$ to "break" the network of particle contacts. The extra displacement of particles and the associated lower shear stress indicate that each layer of particles may move up to an extra $0.1d$ relative to the layer farther from the shear surface before the network reforms. Repeated reversals of the shear direction can be used to compact the network.

We thank Don Martin and Gene Kwon for help with building our experimental setup, and Ricardo Pizarro for assistance in the height measurements. This work was supported by NASA Grant No. NAG-32736.

*Electronic address: wlosert@glue.umd.edu

[1] S. J. Friedmann, G. Kwon, and W. Losert, J. Geophys. Res. **108**, 2380 (2003).
[2] W. Losert, L. Bocquet, T. C. Lubensky, and J. P. Gollub, Phys. Rev. Lett. **85**, 1428 (2000).
[3] E. Clement, Curr. Opin. Colloid Interface Sci. **4**, 294 (1999).
[4] R. A. Bagnold, Proc. R. Soc. London A **225**, 49 (1954); **295**, 219 (1966).
[5] J. T. Jenkins and S. B. Savage, J. Fluid Mech. **130**, 187 (1983).
[6] M. Babic, Phys. Fluids **9**, 2486 (1997).
[7] W. Losert and G. Kwon, Adv. Complex Syst. **4**, 369 (2001).
[8] C. Josserand, A. V. Tkachenko, D. M. Mueth, and H. M. Jaeger, Phys. Rev. Lett. **85**, 3632 (2000).
[9] R. P. Behringer, D. Howell, L. Kondic, S. Tennakoon, and C. Veje, Physica (Amsterdam) **133D**, 1 (1999).
[10] D. M. Mueth *et al.*, Nature (London) **406**, 385 (2000).
[11] B. Utter and R. P. Behringer, Eur. Phys. J. E (to be published).
[12] F. Gadala-Maria and A. Acrivos, J. Rheol. (N.Y.) **24**, 799 (1980).
[13] J. B. Knight, C. G. Fandrich, C. N. Lau, H. M. Jaeger, and S. R. Nagel, Phys. Rev. E **51**, 3957 (1995).
[14] J.C. Philippe, Rep. Prog. Phys. **59**, 1133 (1996).